Effect of fibril shape on adhesive properties

Daniel Soto,[1,a)] Ginel Hill,[1] Aaron Parness,[2] Noé Esparza,[2] Mark Cutkosky,[2] and Tom Kenny[2]
[1]*Department of Applied Physics, Stanford University, Stanford, California 94305, USA*
[2]*Department of Mechanical Engineering, Stanford University, Stanford, California 94305, USA*

(Received 17 March 2010; accepted 25 June 2010; published online 2 August 2010)

Research into the gecko's adhesive system revealed a unique architecture for adhesives using tiny hairs. By using a stiff material (β-keratin) to create a highly structured adhesive, the gecko's system demonstrates properties not seen in traditional pressure-sensitive adhesives which use a soft, unstructured planar layer. In contrast to pressure sensitive adhesives, the gecko adhesive displays frictional adhesion, in which increased shear force allows it to withstand higher normal loads. Synthetic fibrillar adhesives have been fabricated but not all demonstrate this frictional adhesion property. Here we report the dual-axis force testing of single silicone rubber pillars from synthetic adhesive arrays. We find that the shape of the adhesive pillar dictates whether frictional adhesion or pressure-sensitive behavior is observed. This work suggests that both types of behavior can be achieved with structures much larger than gecko terminal structures. It also indicates that subtle differences in the shape of these pillars can significantly influence their properties. © *2010 American Institute of Physics*. [doi:10.1063/1.3464553]

The frictional adhesion property of gecko tissue was discovered by simultaneously measuring the shear and normal forces generated during adhesion.[1] The shear and normal forces produced by synthetic gecko adhesives, however, are infrequently tested.[2,4–6] While many adhesives have used small fibrillar structures to create adhesion, only a few adhesives have demonstrated this frictional adhesion property.[2,5,7] We have previously developed a fibrillar adhesive that displays frictional adhesion using tapered triangular wedge structures measuring 20 μm by 20 μm at the base by 60 μm in height. These were created by casting polydimethylsiloxane (PDMS) silicone rubber (Young's modulus ~2 MPa) in a microfabricated mold.[5] A single tapered pillar is shown in Fig. 1. We fabricated nontapered pillars with similar dimensions and compliance to test the effect of pillar geometry on the adhesive properties. A nontapered pillar is shown in Fig. 1. To understand how pillar shape influences adhesive behavior, we isolate single adhesive pillars and test their adhesive properties using a micromechanical force sensor that can simultaneously measure force along two axes at the micronewton (μN) scale. Understanding how fibril shape affects the adhesive properties will help in the creation of fibrillar adhesives with customized properties.

To characterize the adhesive properties, we determine the set of shear and normal force pairs for which stable attachment is possible. We use a flat-tipped piezoresistive cantilever capable of simultaneously measuring forces along two orthogonal axes to measure the forces at the adhesive interface. The dual-axis cantilever utilized is described in Refs. 8 and 9 and is depicted in Fig. 2. This sensor is a microfabricated silicon cantilever with implanted piezoresistive regions that form strain sensors that change resistance when the cantilever is deflected. It is similar to an atomic force microscope cantilever but instead of a sharp tip, this sensor has a 20×40 μm^2 platform for the pillar to adhere to and its unique geometry enables simultaneous detection of normal and shear forces applied at the tip. The change in resistance is sensed by a Wheatstone bridge signal conditioning circuit and converted to a voltage. The structure is designed so that the members used to sense normal forces are stiff in the shear direction and vice versa to minimize crosstalk between the two axes. To calibrate the sensor, we measure the displacement sensitivity of the cantilever and signal conditioning circuit directly, and then estimate the cantilever's stiffness using a combination of resonant frequency measurement, finite-element modeling, and interaction measurements with a reference cantilever.[10] The cantilever has a normal spring constant of 0.7 N/m and a shear spring constant of 3.9 N/m.

The adhesive pillar and cantilever are placed in a custom system that allows for alignment of the pillar and cantilever, motion control, and force data collection. Figure 2 shows the relative orientations of the cantilever and pillar, the convention for forces on the cantilever, and the directions of pillar motion during the test. The cantilever approaches the tip, makes contact, and applies compressive stress to the interface. In these tests, we apply compressive forces of 1–5 μN. After the compression phase, the cantilever is

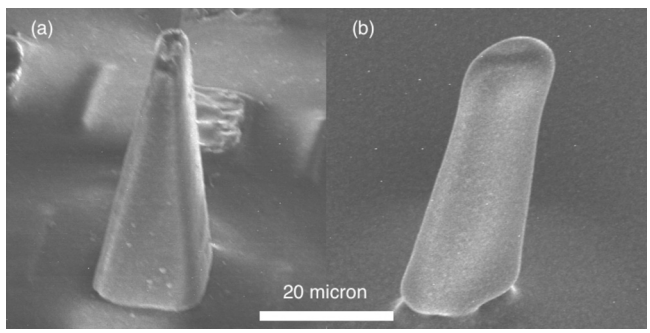

FIG. 1. Scanning electron microscopy images of pillar types. Both pillars share a base width of ~20 μm and a height of ~60 μm. The pillar in (a) is ~20 μm thick at the base and tapers to a tip. The pillar in (b) is ~12 μm thick at the base and has uniform thickness along the length of the beam.

[a)]Electronic mail: dsoto@stanford.edu.

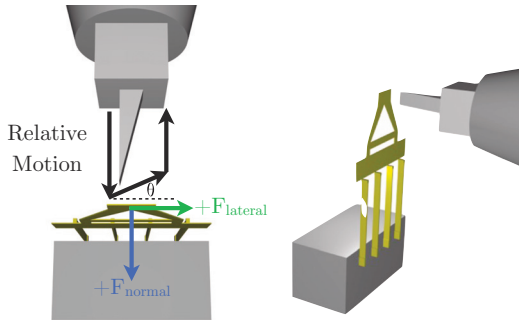

FIG. 2. (Color) Diagram of mounted pillar and force-sensing cantilever. The black arrows indicate the relative motion of the pillar and cantilever. The blue and green arrows indicate the direction of positive forces exerted on the cantilever. This convention is used in the force plots.

withdrawn from the pillar along a straight line at an angle θ to the cantilever surface (Fig. 2). The angle θ varies from 0° to 90° to provide loads varying between primarily shear and primarily normal. For high shear loads, the pillar is deflected and the side of the pillar contacts the substrate. We find the forces present at the moment of failure by analyzing the force trace data (Fig. 3). The stresses at the interface increase until the interface breaks, at which point the measured forces either decrease rapidly or level off. Failure can be either a vertical detachment from the surface or a slipping failure while the pillar is still in contact. The normal and shear forces at these failure events are plotted as points in force space with normal force on the vertical axis and shear force on the horizontal axis. When these points are plotted together, they create a limit surface[11] that separates force pairs with stable attachment from force pairs that will detach.

The dimensions of the nontapered pillar were chosen to match the height (60 μm) and width (20 μm) of the tapered pillar. The thickness (12 μm) was chosen to provide more lateral compliance (0.03 N/m) than the tapered pillar (0.15 N/m). These compliances allow both pillars to make side contact with the cantilever. In Fig. 4, we see the limit surface

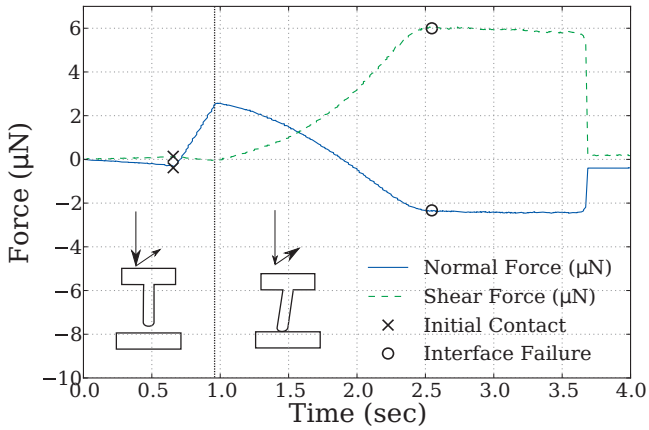

FIG. 3. (Color) Adhesion test data. There are two phases to this test. To the left of the vertical dotted line, the pillar is approaching the cantilever. To the right of the line, the pillar is being retracted at an angle. From t=0 to the initial contact point, there is a signal drift likely due to charge on the PDMS sample. Between the initial contact and peak compression point, the cantilever stage approaches the sample applying positive normal force to the cantilever. After the peak compression, the stage is moved in both the normal and shear directions to generate forces in both axes. In this case, change in the slopes of the forces show an adhesive failure. The forces at this interface failure are recorded for plotting in the limit surface.

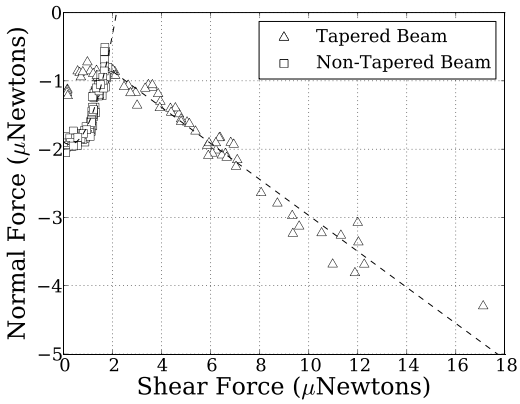

FIG. 4. Limit surfaces for tapered and nontapered single pillars. Each data point reports the forces preceding a single failure event. Trials are run at 19 pull angles ranging between 0° (shear) and 90° (vertical). Each of these angles is tested at two different levels of peak compressive load. Parabolic and linear fits are included as a guide to the eye.

of a tapered pillar and a nontapered pillar. These limit surfaces show that the tapered pillar exhibits a gecko-like frictional adhesion behavior while the nontapered pillar exhibits pressure-sensitive adhesive behavior.[1]

The nontapered pillar displays the same behavior that is observed in a soft hemispherical contact. The behavior of a hemispherical contact under shear and normal forces is modeled by Savkoor and Briggs.[12] This model predicts the normal force to be a quadratic function of the shear force at the interface. This parabolic shape is consistent with failure data we observe in the nontapered beam but we believe the mechanism is different. This adhesive behavior is also observed in familiar pressure-sensitive adhesives such as tape or rubber cement. The tapered pillar displays a different limit surface than the single nontapered element (Fig. 4). Although the limit curve is initially parabolic like the Savkoor–Briggs surface, there is an inflection point after which the curve displays frictional adhesion behavior. The differences in the behavior of the pillars can be explained using the peel-zone adhesion model presented by Tian[13] together with an elastica model[14] of the tapered pillar deformation.

The peel-zone model of adhesion proposes that for a bent flexible pillar the shear force for an adhesive contact is generated by the area in intimate contact while the normal force is generated from the area where the pillar is peeling away from the substrate. The peel zone geometry applies to our situation in that when the pillar is sufficiently sheared by the cantilever, the tip of the pillar is bent so that a length of the flat section of the pillar is in side contact. Glassmaker and Hui[15] show that for a beam in a similar geometry that the radius of curvature in this peel zone is an increasing function of the moment of inertia of the beam. To achieve larger shear forces, the length of side contact must increase. Due to the taper, the thickness and moment of inertia of the pillar at the peel-zone increases and the radius of curvature at the point of peeling increases. As this radius increases, the length of the zone close enough for attractive force increases, allowing for more normal adhesion and the adhesive demonstrates frictional adhesion. In contrast, the nontapered beam has a uniform moment of inertia and does not show the increase in normal force with increasing shear force.

These results suggest that by tailoring the pillar shape such that the local radius of curvature at the point of contact

is an increasing function of shear load, frictional adhesion can be achieved. While the geometries are very different, the tokay gecko adhesive behaves in a similar fashion. The initial contact of the gecko adhesive is with the flat edges of the spatulae. With shear loading, the spatulae are bent into flat contact resulting in a large increase in shear adhesion. We must be cautious in using this beam model to explain gecko adhesion but we do observe similarities in these very simple tapered structures.

Experimental and modeling results suggest that side contact is important for shear adhesion and enhanced friction.[16] The adhesives in the literature that demonstrate this side contact are nanoscale high-aspect-ratio structures such as carbon nanotubes or polypropylene nanohairs.[2,7] This work shows that side contact and its adhesive benefits are possible in structures much larger and with smaller aspect ratios than carbon nanotubes or polymer nanorods. This suggests that a wide range of materials and dimensions may be used to create adhesives that mimic the gecko's property of frictional adhesion.

The variation in adhesive performance in these pillars suggests that fibrillar adhesive properties can be designed to match the application. Researchers have investigated the effect of tip shape on the amount of normal adhesion measured.[3,17] This study adds to these efforts by examining the shape of the pillar and its influence on the adhesive property demonstrated. By tailoring both the tip and pillar shape, both the amount of adhesion and the type of adhesion generated can be tuned to fit the application. Pillars displaying frictional adhesion are appropriate for applications such as clean manufacturing grippers that require shear loading or easy detachment.[18] For applications requiring infrequent detachment, or where normal force is more important than shear force, pillars displaying pressure-sensitive behavior may be more appropriate. Thorough investigations of other uniform and nonuniform pillars and their adhesive properties will provide a basis for the design of fibrillar adhesives for specific applications.

[1]K. Autumn, A. Dittmore, D. Santos, M. Spenko, and M. R. Cutkosky, J. Exp. Biol. **209**, 3569 (2006).
[2]J. Lee, R. S. Fearing, and K. Komvopoulos, Appl. Phys. Lett. **93**, 191910 (2008).
[3]S. Gorb, M. Varenberg, A. G. Peressadko, and J. Tuma, J. R. Soc., Interface **4**, 271 (2007).
[4]M. Varenberg and S. Gorb, J. R. Soc., Interface **4**, 721 (2007).
[5]A. Parness, D. R. Soto, N. Esparza, N. Gravish, M. Wilkinson, K. Autumn, and M. R. Cutkosky, J. R. Soc., Interface **6**, 1223 (2009).
[6]M. P. Murphy, B. Aksak, and M. Sitti, Small **5**, 170 (2009).
[7]L. Qu, L. Dai, M. Stone, Z. Xia, and Z. L. Wang, Science **322**, 238 (2008).
[8]B. Chui, T. Kenny, H. Mamin, B. Terris, and D. Rugar, Appl. Phys. Lett. **72**, 1388 (1998).
[9]K. Autumn, Y. Liang, S. Hsieh, W. Zesch, W. Chan, T. Kenny, R. S. Fearing, and R. J. Full, Nature (London) **405**, 681 (2000).
[10]G. Hill, Ph.D. thesis, Stanford University, 2009.
[11]S. Goyal, A. Ruina, and J. Papadopoulos, Wear **143**, 307 (1991).
[12]A. Savkoor and G. Briggs, Proc. R. Soc. London, Ser. A **356**, 103 (1977).
[13]Y. Tian, N. Pesika, H. Zeng, K. Rosenberg, and B. Zhao, Proc. Natl. Acad. Sci. U.S.A. **103**, 19320 (2006).
[14]R. Frisch-Fay, *Flexible Bars* (Butterworths, London, 1962).
[15]N. Glassmaker and C.-Y. Hui, J. Appl. Phys. **96**, 3429 (2004).
[16]B. Schubert, C. S. Majidi, R. E. Groff, S. Baek, B. Bush, R. Maboudian, and R. S. Fearing, J. Adhes. Sci. Technol. **21**, 1297 (2007).
[17]A. del Campo, C. Greiner, and E. Arzt, Langmuir **23**, 10235 (2007).
[18]H. Jeong, J. Lee, H. Kim, S. Moon, and K. Suh, Proc. Natl. Acad. Sci. U.S.A. **106**, 5639 (2009).